A Generalized Compositional Approach for Reservoir Simulation

Larry C. Young, SPE, Amoco Production Co.
Robert E. Stephenson, SPE, Amoco Production Co.

Abstract

A procedure for solving compositional model equations is described. The procedure is based on the Newton-Raphson iteration method. The equations and unknowns in the algorithm are ordered in such a way that different fluid property correlations can be accommodated readily. Three different correlations have been implemented with the method. These include simplified correlations as well as a Redlich-Kwong equation of state (EOS). The example problems considered are (1) a conventional waterflood problem, (2) displacement of oil by CO_2, and (3) the displacement of a gas condensate by nitrogen. These examples illustrate the utility of the different fluid-property correlations. The computing times reported are at least as low as for other methods that are specialized for a narrower class of problems.

Introduction

Black-oil models are used to study conventional recovery techniques in reservoirs for which fluid properties can be expressed as a function of pressure and bubble-point pressure. Compositional models are used when either the in-place or injected fluid causes fluid properties to be dependent on composition also. Examples of problems generally requiring compositional models are (1) primary production or injection processes (such as nitrogen injection) into gas condensate and volatile oil reservoirs and (2) enhanced recovery from oil reservoirs by CO_2 or enriched gas injection. With deeper drilling, the frequency of gas condensate and volatile oil reservoir discoveries is increasing. The drive to increase domestic oil production has increased the importance of enhanced recovery by gas injection. These two factors suggest an increased need for compositional reservoir modeling. Conventional reservoir modeling is also likely to remain important for some time.

0197-7520/83/0101-0516$00.25

In the past, two separate simulators have been developed and maintained for studying these two classes of problems. This result was dictated by the fact that compositional models have generally required substantially greater computing time than black-oil models. This paper describes a compositional modeling approach useful for simulating both black-oil and compositional problems. The approach is based on the use of explicit flow coefficients.

For compositional modeling, two basic methods of solution have been proposed. We call these methods "Newton-Raphson"[1,2] and "non-Newton-Raphson"[3-5] methods. These methods differ in the manner in which a pressure equation is formed. In the Newton-Raphson method the iterative technique specifies how the pressure equation is formed. In the non-Newton-Raphson method, the composition dependence of certain terms is neglected to form the pressure equation. With the non-Newton-Raphson methods, three to eight iterations have been reported per time step.[4,5] Our experience with the Newton-Raphson method indicates that one to three iterations per time step normally is sufficient. In the present study a Newton-Raphson iteration sequence is used. The calculations are organized in a manner which is both efficient and for which different fluid property descriptions can be accommodated readily.

Early compositional simulators were based on K-values that were expressed as a function of pressure and convergence pressure. A number of potential difficulties are inherent in this approach.[6] More recently, cubic equations of state such as the Redlich-Kwong[7] or Peng-Robinson[8] appear to be more popular for the correlation of fluid properties. EOS's like these offer many advantages for the development of generalized fluid property correlations.[9,10] However, matching the EOS to actual fluid systems that develop in porous media has yet to be

demonstrated for some recovery processes. For the simulation of simple black-oil problems, this type of correlation method is very costly. For these reasons, we feel that a compositional model should not be tied exclusively to this type EOS. Black-oil problems can be simulated accurately and at much less cost using two components, K-values that are a function of pressure only, and viscosities and densities based on simple mixing rules. Calculations presented in this paper suggest that a three-component system with composition-dependent K-values that obey Hand's rule[11,12] can be used to simulate some multiple-contact miscible displacements.

Compositional Model Equations

The equations governing multicomponent multiphase flow in porous media arise from three sources[13]: (1) differential material balances describing component flow, (2) phase equilibrium relationships, and (3) constraint equations that require the phase saturations to sum to unity and the mass or mole fraction in each phase to sum to unity.

For simplicity of development, we will neglect dispersion, capillary, and gravity forces; however, the method of solution is applicable to these cases. We also restrict the development to an aqueous phase composed of only one component and two hydrocarbon phases consisting of n components. The hydrocarbon phases could consist of a liquid and a gas or of two liquid phases. We denote these two phases by subscripts o and g.

Under these assumptions, the material balance on the aqueous component is

$$\phi\frac{\partial W}{\partial t}=\nabla\cdot\lambda_w\nabla p+q_w. \quad \ldots\ldots\ldots\ldots\ldots\ldots (1)$$

The material balances on the components of the hydrocarbon phases are

$$\phi\frac{\partial Fz_i}{\partial t}=\nabla\cdot(\lambda_o x_i+\lambda_g y_i)\nabla p+q_i \quad \ldots\ldots\ldots\ldots (2)$$

for $i=1 \ldots n$. The phase equilibrium relationships can be expressed in terms of the equality of fugacities as

$$f_{oi}=f_{gi};\ i=1 \ldots n \quad \ldots\ldots\ldots\ldots\ldots\ldots (3a)$$

or by the use of equilibrium K-values as

$$y_i=K_i x_i;\ i=1 \ldots n. \quad \ldots\ldots\ldots\ldots\ldots\ldots (3b)$$

The constraint equations are

$$\sum_{i=1}^{n} x_i=1, \quad \ldots\ldots\ldots\ldots\ldots\ldots\ldots\ldots (4a)$$

$$\sum_{i=1}^{n} y_i=1, \quad \ldots\ldots\ldots\ldots\ldots\ldots\ldots\ldots (4b)$$

$$\sum_{i=1}^{n} z_i=1, \quad \ldots\ldots\ldots\ldots\ldots\ldots\ldots\ldots (4c)$$

and

$$S_o+S_g+S_w=1. \quad \ldots\ldots\ldots\ldots\ldots\ldots\ldots\ldots (4d)$$

The saturation constraint, Eq. 4d, can be expressed alternatively as

$$1-F\left[\frac{(1-v)}{\rho_o}+\frac{v}{\rho_g}\right]-\frac{W}{\rho_w}=0. \quad \ldots\ldots\ldots\ldots (4e)$$

Since the overall composition is defined by

$$z_i=(1-v)x_i+vy_i;\ i=1 \ldots n, \quad \ldots\ldots\ldots\ldots\ldots (5)$$

only two of the three composition constraints, Eq. 4, are linearly independent. Eqs. 1 through 5 may be viewed as $3n+4$ linearly independent equations in the $3n+4$ unknowns: x_i, y_i, z_i, F, W, v, and p, where functional relationships for λ_o, λ_g, λ_w, ρ_o, ρ_g, ρ_w, and f_{oi} and f_{gi} or K_i in terms of these variables are assumed to exist.

An overall hydrocarbon balance can be derived from these equations by summation of Eq. 2 over i together with the use of the constraints, Eq. 4 by

$$\phi\frac{\partial F}{\partial t}=\nabla\cdot(\lambda_o+\lambda_g)\nabla p+q_f. \quad \ldots\ldots\ldots\ldots\ldots (6)$$

This derivation implies that any n of the $n+1$ equations, Eq. 2 and Eq. 6, are linearly independent. For the development that follows, we choose the first $n-1$ of Eq. 2 and Eq. 6 as our linearly independent set.

By the use of finite difference approximations for the material balance equations, the problem can be reduced to an algebraic one for each time step. The discretized material balance equations for gridpoint j can be expressed by the hydrocarbon component balance

$$V_j'[(Fz_i)_j^{m+1}-(Fz_i)_j^m]+\sum_{k=1}^{N} T_{ijk}p_k^{m+1}=Q_{ij},$$
$$i=1 \ldots n-1, \quad \ldots\ldots\ldots\ldots\ldots\ldots (7a)$$

the hydrocarbon overall balance,

$$V_j'(F_j^{m+1}-F_j^m)+\sum_{k=1}^{N} T_{fjk}p_k^{m+1}=Q_{fj}, \quad \ldots\ldots (7b)$$

or the water balance,

$$V_j'(W_j^{m+1}-W_j^m)+\sum_{k=1}^{N} T_{wjk}p_k^{m+1}=Q_{wj}, \quad \ldots\ldots (7c)$$

where $j=1 \ldots N$. The value of the right-side vectors, Q, are established by the well rates and other boundary conditions. If these conditions involve pressure, then this dependence can be incorporated into the flow coefficient arrays. Since explicit flow coefficients have been assumed, the arrays T_i, T_f, and T_w are calculated from conditions at time level m. These arrays are sparse and are determined by the finite-difference operator being us-

ed (e.g., five-point or nine-point). Equations of the same structure as Eq. 7 are obtained with finite-element methods provided the mass or capacity matrix is lumped.[14] In the following, we consider the solution of the algebraic problem consisting of the discretized material balance equations, Eq. 7, the phase equilibrium relationships, Eq. 3, and the constraint equations, Eq. 4. The phase equilibrium and constraint equations must hold at every grid node in the system.

Solution

Fussell and Yanosik[15] created the term "Minimum Variable Newton-Raphson" (MVNR) for an iteration procedure for single-cell calculations. Fussell and Fussell[1] extended this procedure for compositional modeling. When the Newton-Raphson method is applied to the foregoing equations, the Jacobian matrix is sparse. The basic idea behind the minimum variable procedure is to exploit the sparse structure of this Jacobian. The procedure described here differs from that of Fussell and Fussell in the ordering of the equations and unknowns. The ordering we propose results in computations that are efficient, and it permits different fluid property correlations to be implemented readily within a single simulator. The procedure is described first for the case in which K-values can be expressed as functions of pressure only or of pressure and overall composition. Next, the procedure is described for the case when the phase equilibrium relationships are dependent on individual phase compositions.

K-Values a Function of Pressure and Overall Composition

For a given timestep the problem has been reduced to one of solving for the $N(3n+4)$ unknowns,

$$x_{ij}^{m+1}, y_{ij}^{m+1}, z_{ij}^{m+1}, v_j^{m+1}, F_j^{m+1}, W_j^{m+1}, p_j^{m+1},$$

where $i=1 \ldots n$ and $j=1 \ldots N$. For convenience, whenever the subscript on v, F, W, and p and the second subscript on x, y, and z does not appear, it will be implied. Similarly, the superscript $m+1$ will be implied whenever absent.

In Appendix A, it is shown that with the assumption of K-values dependent only on pressure and overall composition, z_n, x_i, and y_i can be simply expressed in terms of v, p, and z_i by using Eqs. 3b, 4c, and 5. The remaining variables are solved for using a combination of Eqs. 4a, 4b, and 5 by

$$\sum_{i=1}^{n} (y_i - x_i) = \sum_{i=1}^{n} \frac{(K_i-1)z_i}{1+(K_i-1)v} = 0, \quad \ldots\ldots\ldots (8)$$

the discretized material balance equations, Eq. 7, and the saturation constraint equation, Eq. 4e. For each iteration, these equations are linearized as described in Appendix A. After linearization the equations are formulated in terms of the change in the unknowns over the iteration. Eq. 8 is then approximated by

$$a_{vj}\Delta v_j + \sum_{i=1}^{n-1} a_{ij}\Delta z_{ij} + a_{pj}\Delta p_j = r_{vj}, \quad \ldots\ldots\ldots (9)$$

for $j=1 \ldots N$, where Δ denotes the change over an iteration. For a gridpoint with only a single hydrocarbon phase, Eq. 9 reduces to $\Delta v_j = 0$. The material balance equations, Eq. 7, become

$$V_j'(F_j\Delta z_{ij} + z_{ij}\Delta F_j) + \sum_{k=1}^{N} T_{ijk}\Delta p_k = r_{ij},$$

$$i=1 \ldots n-1, \quad \ldots\ldots\ldots\ldots\ldots (10a)$$

$$V_j'\Delta F_j + \sum_{k=1}^{N} T_{fjk}\Delta p_k = r_{fj}, \quad \ldots\ldots\ldots\ldots (10b)$$

and

$$V_j'\Delta W_j + \sum_{k=1}^{N} T_{wjk}\Delta p_k = r_{wj}, \quad \ldots\ldots\ldots\ldots (10c)$$

for $j=1 \ldots N$. The linearized saturation constraint, Eq. 4e, is

$$c_{vj}\Delta v_j + \sum_{i=1}^{n-1} c_{ij}\Delta z_{ij} + c_{fj}\Delta F_j + c_{wj}\Delta W_j + c_{pj}\Delta p_j = r_{pj}, \quad \ldots\ldots\ldots\ldots\ldots (11)$$

for $j=1 \ldots N$. To illustrate the method of solving Eqs. 9 through 11, the unknowns are combined into a single vector, which we denote by $\Delta\Psi$, in the following order: Δv, Δz_1, $\Delta z_2 \ldots \Delta z_{n-1}$, ΔF, ΔW, Δp. The equations are ordered as they appear here, and all coefficients are combined into a Jacobian matrix. For each iteration, the algebraic problem can be expressed by

$$J\,\Delta\Psi = r, \quad \ldots\ldots\ldots\ldots\ldots\ldots\ldots\ldots (12)$$

where J and r are the Jacobian and the negative of the residual vector, respectively.

For a one-dimensional (1D) problem with five gridpoints ($N=5$) and three hydrocarbon phase components ($n=3$), the structure of the Jacobian matrix is illustrated in Fig. 1, from which it is apparent that the Jacobian is quite sparse. The algebraic problem can be expressed more conveniently in terms of a Jacobian matrix partitioned into $N \times N$ blocks. The structure of this block Jacobian is illustrated in Fig. 2. Some of the elements are

$$(B_f)_{jk} = \delta_{jk} V_j' F_j,$$

$$(B_i)_{jk} = \delta_{jk} V_j' z_{ij},$$

$$(B)_{jk} = \delta_{jk} V_j',$$

$$(C_w)_{jk} = \delta_{jk} c_{wj} = -\delta_{jk} \left(\frac{1}{\rho_w}\right)_j,$$

and

$$(C_f)_{jk} = \delta_{jk} c_{fj} = -\delta_{jk} \left[\frac{(1-v)}{\rho_o} + \frac{v}{\rho_g}\right]_j. \quad \ldots\ldots (13)$$

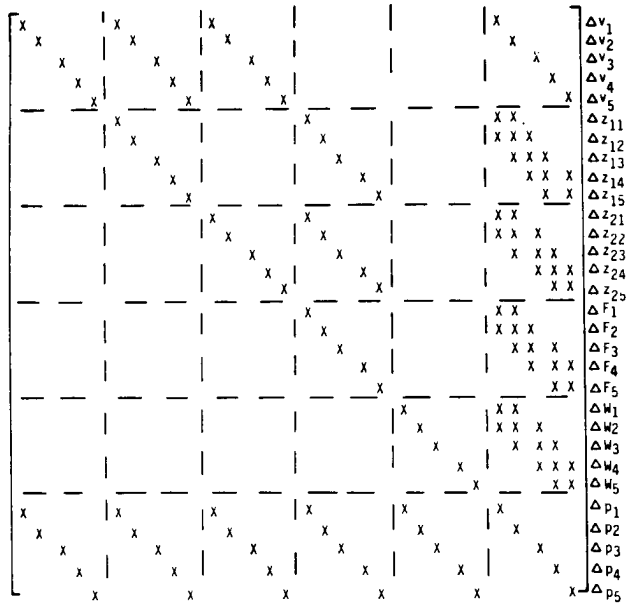

Fig. 1—Structure of Jacobian for 1D problem with five gridpoints ($N=5$) and three hydrocarbon phase components ($n=3$).

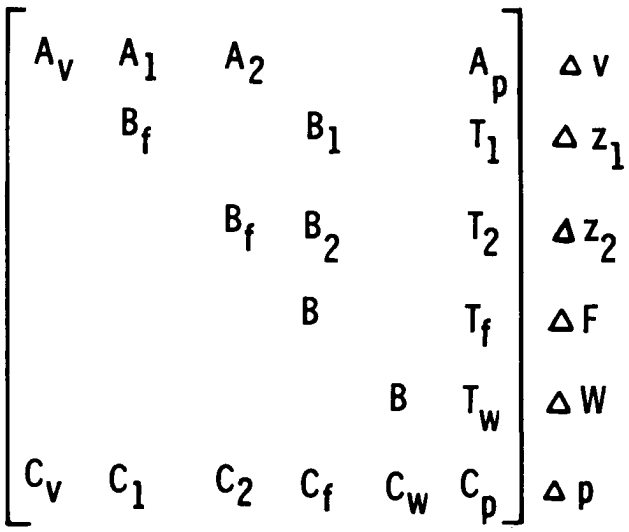

Fig. 2—Structure of Jacobian partitioned into *N*x*N* blocks for *K*-values a function of pressure and overall composition.

The relationship between the other elements of the block Jacobian, indicated by upper-case letters, and the corresponding variables in Eqs. 9 through 11, indicated by lower-case variables, is the same as that for the elements listed in Eq. 13. T_{ijk}, T_{fjk}, and T_{wjk} are the same as in Eqs. 7 and 10. Each element of the block Jacobian is itself a diagonal matrix except for T_i, T_f, and T_w—i.e., the only internodal dependence of the equations comes through the flow terms. Fig. 1 indicates that for a 1D problem these blocks are tridiagonal, while in general they will reflect the difference formula used.

The solution of the equations over time is outlined as follows.

1. The pressure, water saturation, and overall hydrocarbon composition at each gridpoint are specified as initial conditions.

2. The hydrocarbon is flashed at the initial conditions and Eq. 4e is applied to determine the composition and quantity of the hydrocarbon phases, and the phase densities. The coefficients of Eqs. 9 and 11 are calculated, and Eq. 9 is used to eliminate Δv from Eq. 11.

3. Viscosities and relative permeability are calculated and the coefficients of Eq. 10 are determined.

4. The problem is reduced to one with only pressure as an unknown by using Eq. 10 to eliminate Δz_i, ΔF, and ΔW from Eq. 11 (see Fig. 2).

5. The equation for pressure is solved. For multidimensional problems, we use line successive overrelaxation[16] for this step, but other methods also could be used.

6. Back substitution is used to solve Eq. 10 for ΔW, ΔF, and Δz_i. In the back substitution for Δz_i, the updated value of F is used in Eq. 10a. By this technique Eq. 7a is satisfied exactly for every iteration.

7. Back substitution is used to solve Eq. 9 for Δv.

8. The hydrocarbon is flashed at the updated composition and pressure to determine refined estimates of v, x_i, and y_i. Updated phase densities and coefficients of Eqs. 9 and 11 are calculated. Eq. 9 is used to eliminate Δv from Eq. 11.

9. The residual of Eq. 4e is used to determine convergence. If a tolerance is exceeded, then B_i, B_f, and the residuals of Eq. 10 are updated and another iteration is performed by returning to Step 4. If the tolerance is met, then a new timestep is started by returning to Step 3.

Since the conditions from the preceding timestep are used as initial estimates for a new timestep, the calculations performed in Step 8 of the preceding timestep need not be repeated for the new timestep.

From Figs. 1 and 2 it is apparent that with this ordering of the equations no fill takes place during the elimination except in element C_p of the block Jacobian. It should also be noted that if only one iteration is performed, this procedure is conceptually the same as the implicit pressure, explicit saturation (IMPES) technique used for black-oil modeling.[17] Furthermore, when a two-component hydrocarbon is used, the number of arithmetic operations is similar to that for an IMPES black-oil model formulation.

Most algorithms for black-oil and compositional modeling solve for one phase saturation using Eq. 4d. Therefore, Eq. 4d is satisfied exactly, while the material balance equations, Eq. 7, are not satisfied exactly. As a result, a material balance error is incurred. In contrast, with the algorithm described in this paper, Eq. 4d or 4e is satisfied to within a prescribed convergence tolerance while Eq. 7 is satisfied exactly. For this reason, no material balance error is incurred other than that caused by a lack of machine precision.

Phase Equilibria a Function of Individual Phase Compositions

As described previously, for a given timestep the algebraic problem consists of solving $N(3n+4)$ equa-

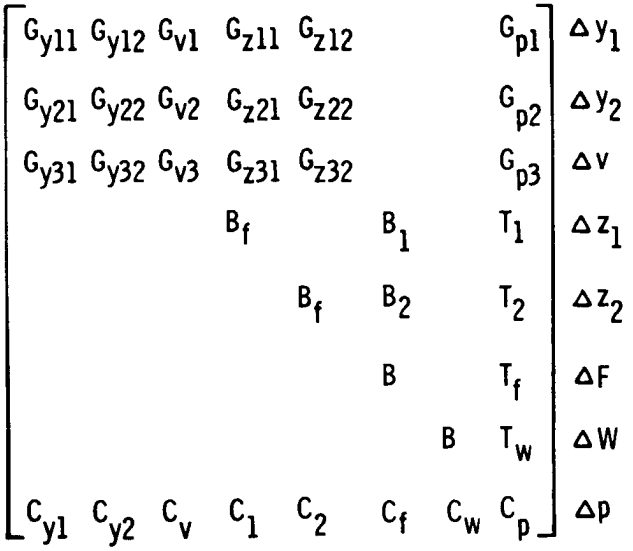

Fig. 3—Structure of Jacobian partitioned into *NxN* blocks for phase equilibria dependent on individual phase compositions.

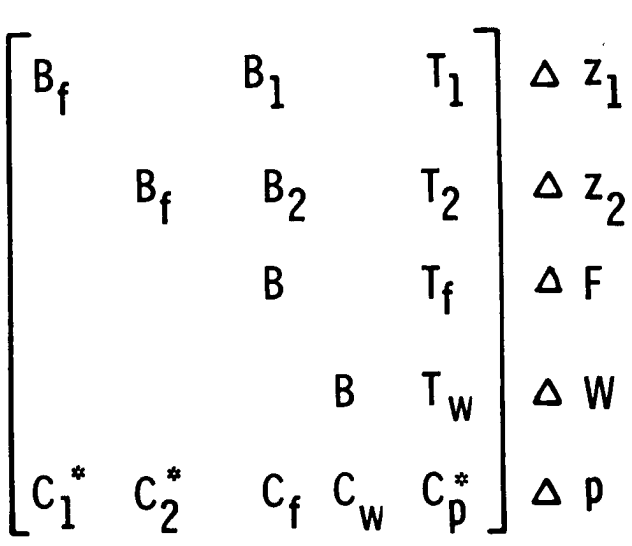

Fig. 4—Structure of block Jacobian after partial forward elimination for any fluid-property correlation.

tions for the unknowns

$$x_{ij}^{m+1}, y_{ij}^{m+1}, z_{ij}^{m+1}, v_j^{m+1}, F_j^{m+1}, W_j^{m+1}, p_j^{m+1},$$

for $i=1 \ldots n$ and $j=1 \ldots N$. For convenience the superscript $m+1$ and subscript denoting gridpoint number will be implied whenever absent. Implementation of the Redlich-Kwong,[7] Peng-Robinson,[8] or a similar EOS in a Newton-Raphson scheme is more complex than for the simplified fluid property correlations described previously. This increased complexity is caused by the dependence of the phase equilibrium relationship, Eq. 3a, on the individual phase compositions x_i and y_i. For this case, x_i, $i=1 \ldots n$, y_n, and z_n can be simply expressed in terms of v, y_i, and z_i, $i=1 \ldots n-1$ by using Eqs. 4a, 4b, and 5. As described in Appendix B, Eq. 3a can be approximated by the linearized equation

$$\sum_{i=1}^{n-1} g_{y\ell ij}\Delta y_{ij} + g_{v\ell j}\Delta v_j + \sum_{i=1}^{n-1} g_{z\ell ij}\Delta z_{ij} + g_{p\ell j}\Delta p_j = r_{y\ell j}, \quad \ldots\ldots\ldots\ldots\ldots\ldots (14)$$

for $\ell=1 \ldots n; j=1 \ldots N$. For any gridpoint with only a single hydrocarbon phase present, these equations reduce to

$$\Delta v=\Delta y_i=0;\ i=1 \ldots n-1.$$

Eq. 10 applies for the linearized material balance equations, since the representation of these equations is independent of the fluid property correlation used. As described in Appendix B, the linearized saturation constraint, Eq. 4e, is

$$\sum_{i=1}^{n-1} c_{yij}\Delta y_{ij} + c_{vj}\Delta v_j + \sum_{i=1}^{n-1} c_{ij}\Delta z_{ij} + c_{fj}\Delta F_j + c_{wj}\Delta W_j + c_{pj}\Delta p_j = r_{pj}. \quad \ldots\ldots (15)$$

If the unknowns are combined into a single vector, $\Delta\Psi$, in the order $\Delta y_1, \Delta y_2 \ldots \Delta y_{n-1}, \Delta v, \Delta z_1, \Delta z_2 \ldots \Delta z_{n-1}, \Delta F, \Delta W, \Delta p$—and the order of the equations is Eq. 14, Eq. 10, and Eq. 15, then for each iteration the algebraic problem can be expressed by Eq. 12. The structure of the block Jacobian is illustrated in Fig. 3. All elements of the block Jacobian are again diagonal matrices except for T_i, T_f, and T_w, which arise from discretization of the flow terms.

The solution of the equations over time is similar to the method outlined previously for K-values dependent on a function of pressure and overall composition with the following exceptions.

A. In Step 2 the coefficients of Eqs. 14 and 15 are calculated, all elements of G_y below the diagonal (see Fig. 3) are eliminated, and these equations are then used to eliminate Δy_i and Δv from the last row, Eq. 15.

B. After Step 3, gridpoints that have been in a single hydrocarbon-phase state are tested by the method described in Appendix B to determine whether they have reverted to a two-phase state. For the new two-phase points, Step A above is completed.

C. In Step 4 the variables are eliminated from Eq. 15 rather than Eq. 11.

D. In Step 7, back substitution in Eq. 14 is used to solve for Δv and Δy_i. Any gridpoint for which v is outside the range of zero to one is considered to have only a single hydrocarbon phase for the remainder of the timestep.

E. In Step 8, updated values of x_i are calculated from Eq. 5, and updated phase densities are calculated. Step A above is completed.

F. In Step 9, a tolerance is used on the error in the phase equilibrium relations in addition to the tolerance on the saturation constraint.

Step B is required here because the detection of gridpoints that change from one- to two-phase requires too much computation to be performed each iteration. Testing for this condition once per timestep has proved to be sufficient. It is important to note that calculations

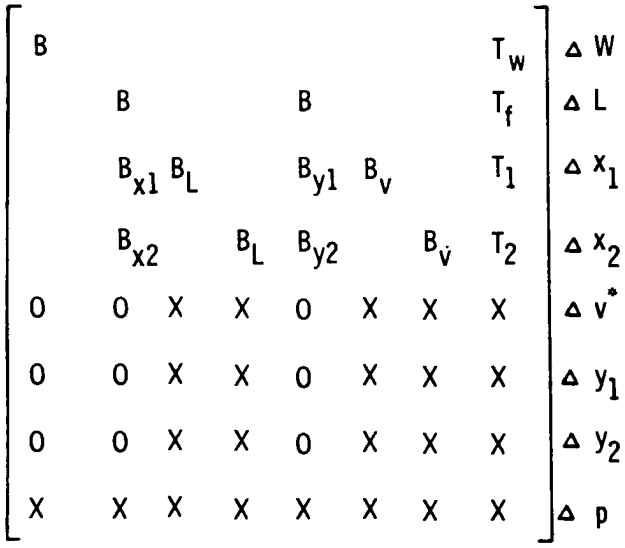

Fig. 5—Structure of block Jacobian for *v-y-p* iteration of Ref. 1.

required for Step E of this procedure are only slightly greater per gridpoint that that required for one Newton-Raphson iteration for a single-cell flash calculation. The following examples illustrate this calculation can be reduced even further by using a procedure that recalculates the Jacobian only at gridpoints that do not meet the convergence criteria.

Generalized Solution Method

From the preceding discussion, it is apparent that similar calculational procedures can be used for vastly different fluid property correlations. The reason this similarity is possible can be found by comparing Figs. 2 and 3. After the partial elimination in Steps 2 and 8 of the calculational procedure outlined previously, the problem has been reduced to one having the same structure as that for a problem having only a single hydrocarbon phase. This structure, which is illustrated in Fig. 4, is independent of the fluid property correlation used. The partial forward elimination does not involve any of the flow terms, so it can be performed for each gridpoint independently. For these reasons, it is not difficult to program different routines that perform the calculations outlined previously in Steps 2 and 8 and the viscosity calculation in Step 3 for various fluid property correlations. These fluid property routines can be made completely interchangeable and transparent to the remainder of the program. Using this scheme we have implemented the following fluid property correlations within one basic simulator: (1) *K*-values expressed as a function of pressure, (2) composition-dependent *K*-values that obey Hand's rule, and (3) Redlich-Kwong EOS. The utility of these different fluid property correlations are illustrated by the example problems that follow.

Relationship to Other Methods

The non-Newton-Raphson methods of Kazemi *et al.*[4] and Nghiem *et al.*[5] differ from the Newton-Raphson method by the manner in which the pressure equation is formed. Both methods neglect all the terms in the linearized saturation constraint, Eq. 11 or 15, that depend on concentration or vapor fraction (i.e., all coefficients except c_f, c_w, and c_p are neglected). The scheme of Kazemi *et al.* is equivalent to one in which ΔF and ΔW are eliminated from this simplified saturation constraint equation; then as they describe, an approximate value of c_p is used on the basis of past iterations. The scheme of Nghiem *et al.* is equivalent to one in which c_w/c_f is approximated by a constant value, ΔF and ΔW are eliminated from the simplified saturation constraint, and then c_p/c_f is approximated by Eq. 17 of their paper. Since both of these techniques neglect the composition-dependent terms in the development of a pressure equation, it can be expected that a larger number of iterations may be required for problems that are highly dependent on composition. For a test problem, Nghiem *et al.* reported an average of 6 iterations per timestep. Kazemi *et al.* reported that 3 to 8 iterations per timestep have been required with their method. These numbers are greater than that required for the Newton-Raphson method we use on the example problems that follow.

Mansoori[18] has reported that the non-Newton-Raphson methods sometimes fail to converge when a transition from one to two hydrocarbon phases is encountered. He proposed a solution to this problem that is equivalent to including c_v along with c_f, c_w, and c_p in the linearization of Eq. 4e. Since with his modification the c_i are neglected, we may anticipate a slow convergence rate when those terms are important.

The principal difference between the Newton-Raphson method just described and the MVNR method described by Fussell and Fussell[1] is the ordering of the equations and unknowns. They solved the problem in terms of total vapor and liquid,

$$v^*=vF$$

and

$$L=(1-v)F,$$

rather than vapor fraction and total hydrocarbon (liquid plus vapor). In addition, they used liquid phase fractions rather than the overall hydrocarbon fractions. They ordered their equations differently, depending on whether a gridpoint was predominantly liquid or predominantly vapor. For the predominantly liquid case they used what was termed a "*v-y-p*" iteration, which consisted of the following ordering of the equations: (1) water balance, (2) overall hydrocarbon balance, (3) $n-1$ component balances, (4) n linearized phase equilibrium relationships, and (5) linearized saturation constraint.

The unknowns were ordered by ΔW, ΔL, Δx_i, Δv^*, Δy_i, Δp. For this ordering the structure of the block Jacobian is illustrated in Fig. 5 for a three-component system. Some of the elements of the Jacobian are

$$(B_L)_{jk}=\delta_{jk}V_j'L_j,$$

$$(B_v)_{jk}=\delta_{jk}V_j'v_j^*,$$

$$(B_{xi})_{jk}=\delta_{jk}V_j'x_{ij},$$

and

$$(B_{yi})_{jk}=\delta_{jk}V_j'y_{ij},$$

while the other elements indicated in Fig. 5 are those already defined. When L and the diagonal elements B_L become small, this ordering results in an ill-conditioned matrix and a different (L-x-p) ordering is required.

By comparing Figs. 3 and 5, we can see the differences between the two techniques. The major difference is that the ordering of phase equilibrium and material balance equations is transposed in the two methods. With the MVNR ordering, the last four rows of the last column in Fig. 5 will fill internally with flow coefficients when the Δx_i are eliminated from the phase equilibrium relationships. This results in more computation than with the method presented in this paper. For a 10-component problem the number of arithmetic operations for the forward elimination and back substitution steps (excluding the pressure solution) is 33% greater if a five-point difference scheme is used and 88% greater if a nine-point scheme is used. Of course, this is only for a relatively small portion of the calculations required for one iteration. A more important problem is that the MVNR ordering causes the flow equations to be interwoven with the phase equilibrium equations. This makes the MVNR method a cumbersome one for the implementation of vastly different fluid property correlations within one general simulator.

Results

To demonstrate the capabilities and limitations of various fluid property correlations, three example problems are considered: (1) waterflooding of a conventional oil reservoir with an initial gas saturation, (2) displacement of a conventional oil by carbon dioxide injection, and (3) displacement of a gas condensate by nitrogen injection. These three problems represent a variety of conventional and unconventional displacement processes.

Three fluid-property correlations are used: (1) K-values expressed as a function of pressure, (2) composition-dependent K-values that obey Hand's rule,[11] and (3) Redlich-Kwong EOS.[7]

For the first two of these correlations, density and viscosity are calculated by using the simple power law relationships

$$\rho_o = \left(\sum_{i=1}^{n} x_i \rho_i^{\alpha} \right)^{1/\alpha}$$

and

$$\rho_g = \left(\sum_{i=1}^{n} y_i \rho_i^{\alpha} \right)^{1/\alpha}, \quad \ldots\ldots\ldots\ldots\ldots\ldots (16)$$

and

$$\mu_o = \left(\sum_{i=1}^{n} x_i \mu_i^{\gamma} \right)^{1/\gamma}$$

and

$$\mu_g = \left(\sum_{i=1}^{n} y_i \mu_i^{\gamma} \right)^{1/\gamma}, \quad \ldots\ldots\ldots\ldots\ldots\ldots (17)$$

where ρ_i and μ_i are functions of pressure only. With the third correlation, the EOS provides the densities, while viscosities are provided by a modification of the Steil-Thodos correlation.[19] For the second example problem, Standing-Katz[20] densities are used in the viscosity correlation for the oil-rich liquid. With this approach, inconsistent viscosity data will result at a critical point;[6] however, this does not appear to cause any difficulties in the simulation. With the Hand's rule correlation, the dependence of K-values on composition is independent of the density correlation. Although this can also result in inconsistent data, we have not observed any difficulties. With these exceptions, the three correlations obey the consistency requirements discussed by Nolen.[6]

Waterflood with Initial Gas Saturation

The first example problem considered is a waterflood of a conventional oil reservoir with an initial gas saturation. The oil is from west Texas and can be characterized by the black-oil properties listed in Table 1. The problem is simulated using a conventional black-oil simulator and a compositional model employing the generalized solution method and K-values expressed as a function of pressure only.

The problem consists of a quadrant of a five-spot pattern with uniform properties. A single areal layer and an 11×11 gridpoint system is assumed. The flow equations are discretized using a standard upstream-weighted five-point difference scheme on a point-distributed grid.[17] The relative permeability data given in Table 2 are used with three-phase data calculated using the method of Stone.[21] The ratio of the wellbore radii to interwell distance is 0.0099. The reservoir is initially at a pressure of 5.17 MPa (750 psi) with a gas saturation of 0.10. Water is injected continuously at a bottomhole pressure of 20.68 MPa (3,000 psi) and the producing bottomhole pressure is maintained at 0.689 MPa (100 psi).

With the compositional approach, the fluid properties in Table 1 were used to calculate the parameters of a two-component hydrocarbon system composed of (1) a light-hydrocarbon component (gas) that is soluble in liquid and (2) a nonvolatile liquid component (dead oil). Taking into consideration the necessary conversions to surface conditions, the density and K-value of the gas component can be calculated as a function of pressure directly from the gas FVF and solution GOR by

$$\rho_1 = \rho_g^* / B_g,$$

and

$$K_1 = 1 + \rho_o^* / (\rho_g^* R_s). \quad \ldots\ldots\ldots\ldots\ldots\ldots (18)$$

Since by assumption the second component is nonvolatile, we have

$$K_2 = 0,$$

$$y_1 = 1,$$

and

$$x_1 = 1/K_1. \quad \ldots\ldots\ldots\ldots\ldots\ldots (19)$$

TABLE 1—FLUID PROPERTIES USED IN WATERFLOOD PROBLEM

Pressure		B_o		μ_o		B_g		μ_g		R_s	
(MPa)	(psi)	(m^3/m^3)	(res bbl/STB)	(mPa·s)	(cp)	(m^3/m^3)	(res bbl/Mscf)	(mPa·s)	(cp)	(m^3/m^3)	(Mscf/STB)
1.03	150	1.075	1.075	2.998	2.998	0.1022	18.21	0.0109	0.0109	17.81	0.100
1.72	250	1.091	1.091	2.740	2.740	0.0601	10.71	0.0110	0.0110	24.04	0.135
3.45	500	1.117	1.117	2.345	2.345	0.0293	5.209	0.0114	0.0114	35.27	0.198
6.89	1000	1.157	1.157	1.930	1.930	0.0131	2.336	0.0126	0.0126	52.90	0.297
10.34	1500	1.195	1.195	1.760	1.760	0.00780	1.390	0.0145	0.0145	69.11	0.388
11.72	1700	1.211	1.211	1.728	1.728	0.00665	1.184	0.0155	0.0155	75.52	0.424
13.79	2000	1.208	1.208	1.774	1.774	0.00541	0.963	0.0170	0.0170	75.52	0.424
17.24	2500	1.204	1.204	1.852	1.852	0.00411	0.732	0.0196	0.0196	75.52	0.424
20.68	3000	1.200	1.200	1.929	1.929	0.00359	0.640	0.0221	0.0221	75.52	0.424

$B_w = 1.0 - 0.00058\ (\text{MPa}^{-1})P$
$\mu_w = 0.7$ mPa·s (0.7 cp)
$\rho_g^* = 0.106$ kg/m^3 (0.0659 lbm/cu ft)
$\rho_o^* = 84.9$ kg/m^3 (53.0 lbm/cu ft)

TABLE 2—RELATIVE PERMEABILITY DATA

Water/Oil Relative Permeability

Water Saturation	Oil Relative Permeability	Water Relative Permeability
0.200	1.0000	0.0
0.236	0.7300	0.0005
0.271	0.5700	0.0035
0.307	0.4400	0.0100
0.343	0.3330	0.0200
0.379	0.2400	0.0330
0.414	0.1700	0.0490
0.450	0.1180	0.0690
0.486	0.0810	0.0950
0.521	0.0530	0.1280
0.557	0.0330	0.1690
0.593	0.0180	0.2230
0.629	0.0073	0.2870
0.664	0.0022	0.3700
0.682	0.0010	0.4160
0.700	0.0	0.4700

Gas/Oil Relative Permeability

Gas Saturation	Oil Relative Permeability	Gas Relative Permeability
0.0	1.0000	0.0
0.02	0.7710	0.0
0.05	0.5220	0.0060
0.10	0.2393	0.0245
0.15	0.1423	0.0465
0.20	0.0743	0.0693
0.24	0.0399	0.0955
0.26	0.0293	0.1120
0.28	0.0215	0.1315
0.29	0.0184	0.1425
0.30	0.0158	0.1543
0.32	0.0116	0.1811
0.33	0.0099	0.1962
0.34	0.0086	0.2125
0.36	0.0062	0.2494
0.38	0.0046	0.2830
0.40	0.0033	0.3200
0.45	0.0015	0.3925
0.50	0.0	0.4486
0.80	0.0	1.0000

The gas component viscosity is therefore identical to the gas viscosity in Table 1 (i.e., $\mu_1 = \mu_g$). The viscosity of the oil component can be calculated from Eq. 17 by using the gas component viscosity, the oil phase viscosity in Table 1, and the value of x_1 from Eq. 19 by

$$\mu_2 = \left(\frac{\mu_o^\gamma - x_1 \mu_1^\gamma}{1 - x_1} \right)^{1/\gamma}. \quad \ldots\ldots\ldots\ldots\ldots\ldots (20)$$

Since the oil phase density is given by

$$\rho_o = \frac{\rho_g^* R_s + \rho_o^*}{B_o}, \quad \ldots\ldots\ldots\ldots\ldots\ldots\ldots\ldots (21)$$

the density of component 2 can be calculated by a procedure analogous to that used for calculating viscosity. These relationships were used together with values of

$$\alpha = 1$$

and

$$\gamma = -0.25$$

to correlate the properties in Table 1. Note that mass fractions and mass densities are used consistently in the above equations. It is difficult to correlate the density of real oils using Eq. 16 with molar fractions and densities. This does not decrease the generality of our method, because the representation of the compositional model equations is not dependent on whether mass or molar units are employed.

The waterflooding problem just described involves reservoir repressuring. To simulate this problem with a black-oil model, a variable bubble-point calculation is required. The black-oil model used in this comparison employs a variable bubble-point calculation similar to that described by Thomas *et al.*[22] With a compositional approach, no special provisions are required for the repressurization problem. The bubble-point pressure is indirectly determined by the amount of gas component present. Once the pressure exceeds the bubble-point pressure, Eqs. 16 and 17 continue to provide fluid prop-

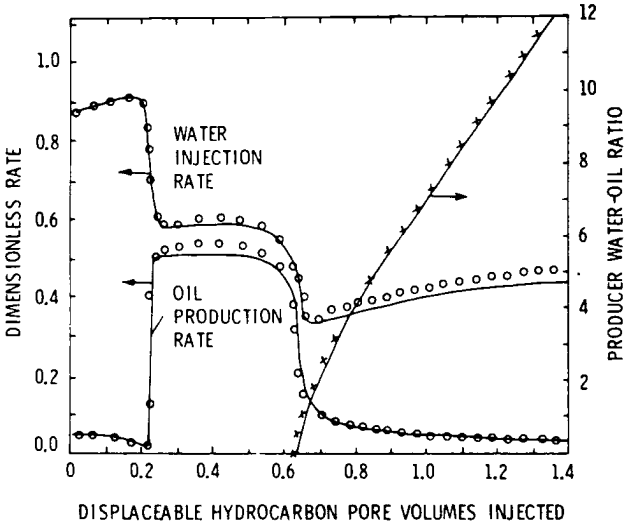

Fig. 6—Calculated results for waterflood problem with initial gas saturation.

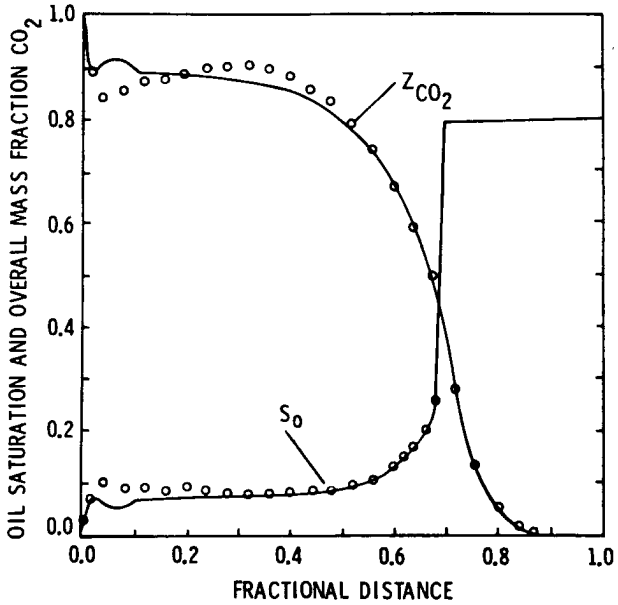

Fig. 7—Profiles of carbon dioxide overall mass fraction and hydrocarbon-rich liquid saturation after 0.6 HCPV injection.

erties that are physically realistic. We feel that this compositional approach is a very natural way to treat reservoir repressuring problems.

From the two approaches, the results for the waterflood problem are illustrated in Fig. 6. In Fig. 6 the production and injection rates are normalized by a characteristic rate which is the steady-state flow rate of a five-spot[23] at floodout conditions (i.e., $S_w=0.7$). From Fig. 6 it is apparent that the compositional approach and black-oil-variable bubble-point approach give similar results. The only appreciable difference is that the compositional model gives rates that are approximately 4% higher than with the black-oil model. This minor discrepancy is caused by the different well correlations used in the two models rather than the fluid-property treatment. The compositional model uses a correlation that relates the bottomhole pressure to the grid pressure at the well location,[24,14] whereas the black-oil model uses a correlation that relates bottomhole pressure to the grid pressures adjacent to the well location. Because of variations in mobility about the producing well, these approaches gave slightly different results. Overall, the agreement is good, and this test confirms that both approaches can give similar results.

Displacement of Oil by CO_2

The second example problem considered is the displacement of a west Texas oil by CO_2. The oil used for this example is the Oil A studied by Turek *et al.*[10] The displacement is simulated using the 17-component Redlich-Kwong fluid-property description developed by Turek *et al.* and by a three-component fluid property description based on Hand's rule.[11]

A 1D displacement was simulated. A temperature of 314.4 K (106°F) was assumed, and an essentially constant pressure of 13.1 MPa (1,900 psi) was used. These conditions correspond to the average conditions for the reservoir from which the fluid was taken. The relative permeabilities used are those in Table 2. The system consisted initially of connate water and oil, with the oil being displaced by continuous CO_2 injection.

At this temperature and pressure, mixtures of Oil A and CO_2 form a single-phase liquid at low CO_2 concentrations and two liquid phases at high concentrations of CO_2. At lower pressures a three-phase (liquid/liquid/vapor) region is encountered, and at still lower pressures a two-phase (liquid/vapor) region exists. This type of phase behavior is typical of west Texas oils at this temperature.

Profiles of oil saturation and CO_2 overall mass fraction are plotted in Fig. 7. Since at this pressure the two hydrocarbon phases are both liquids, we designated the hydrocarbon-rich phase as "oil" and the CO_2-rich phase as "gas." The pseudoternary diagram plotted in Fig. 8 indicates the mechanism by which the displacement process works. From Fig. 8 it is apparent that the original oil composition lies to the right of the critical tie line, while the solvent composition lies to the left. As the CO_2 repeatedly contacts the oil, it vaporizes the light and intermediate components. This enriched CO_2 efficiently displaces the oil. Hutchinson and Braun[25] referred to this process as a vaporization process. Their definitions are convenient to differentiate between processes that are immiscible and those that are multiple-contact miscible. By their definitions, systems that are multiple-contact miscible will revert to a piston-type displacement with no residual oil saturation in the limit of zero dispersion, while systems that are immiscible will revert to a generalized Buckley-Leverett-type displacement in the limit.[26,27] In the example problems, we have used upstream-weighted finite differences with 51 gridpoints. From Fig. 7 it is apparent that the

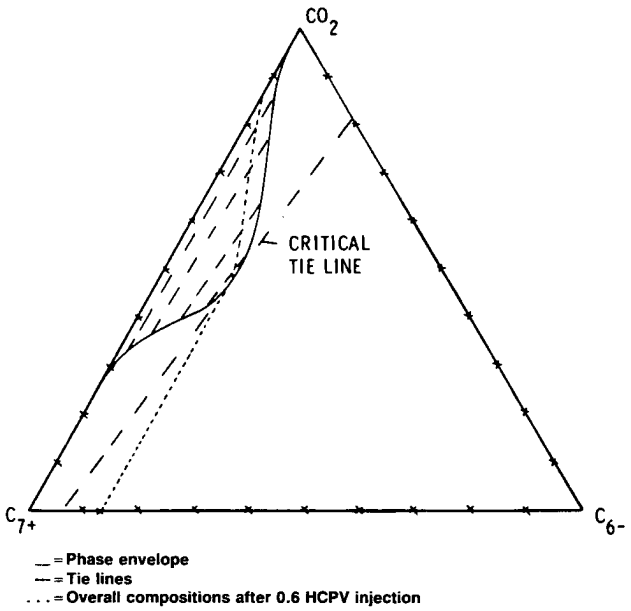

Fig. 8—Ternary diagram of pseudo component mass fractions for carbon dioxide displacement problem.

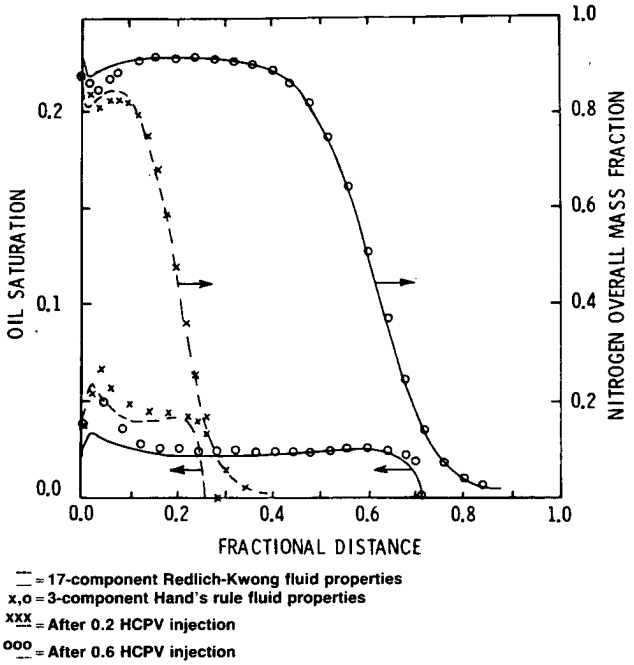

Fig. 9—Profiles of nitrogen overall mass fraction and hydrocarbon liquid saturation for displacement of a gas condensate.

numerical dispersion is sufficient to leave an oil saturation of approximately 10% behind the displacement front. This saturation decreases slowly as the displacement continues or if the number of gridpoints is increased. This observation suggests that the zero dispersion limit is being approached. Unfortunately, there is no way of quantitatively relating the numerical dispersion present in the simulation to the physical dispersion present in reality.

Hutchinson and Braun[25] explained in great length the usefulness and limitations of a ternary representation for processes of this type. They point out that for systems containing more than three components, the diagram obtained will be a function of the manner in which the fluids are contacted. This observation suggests that a ternary representation will not be applicable unless it is constructed through a contacting process similar to that which actually occurs. We have utilized this idea to investigate the possibility of correlating CO_2/oil fluid properties with three pseudocomponents: CO_2, a light-hydrocarbon component, and a heavy-hydrocarbon component. For this investigation, the Redlich-Kwong description of the properties is assumed to be the true case.

From Eq. 2 it is apparent that the sum of several components are governed by the differential material balance that results by summing the equations for the individual components. This observation demonstrates that only as many components need be considered as those required to correlate viscosities, densities, and phase equilibria. When the vapor and liquid compositions that result after various volumes of injection are plotted on one ternary diagram, all give the phase envelope and tie lines in Fig. 8. The phase equilibria can be correlated then, if the diagram in Fig. 8 can be duplicated. The tie lines in Fig. 8 can be described using Hand's rule[11] (i.e., they all intersect at approximately one point). It is not difficult to reproduce the diagram in Fig. 8 by using K-values correlated with the composition variable, u, defined in Eq. A-6. The densities and viscosities that were calculated with the Redlich-Kwong description can be approximated accurately by using Eqs. 16 and 17 with values of $\alpha=-0.5$ and $\gamma=-0.25$. The oil saturation and CO_2 composition profiles calculated by using this three-component description are plotted in Fig. 7. By comparing the profiles in Fig. 7, it is apparent that the three-component description gives a good representation of the fluid properties calculated by the 17-component Redlich-Kwong description.

This work on component lumping is encouraging. The adequacy of the approach also needs to be investigated for conditions in the immiscible regime and for multidimensional problems with significant pressure gradients, since somewhat different composition paths could result in these cases. The calculations do illustrate that three components are sufficient to represent the basic features of the multiple-contact miscible mechanism. For field-scale simulations, the assumption of first-contact miscibility has normally been employed. If more of a mechanistic approach is required for field-scale simulation, then a three-component representation like this one would definitely be superior to the assumption of contact miscibility.

The displacement of Oil A by CO_2 has also been calculated at lower pressures. Whenever the three-phase (liquid/liquid/vapor) region was traversed, meaningful calculations could not be performed because of discontinuous fluid properties that occur as a result of the multiple-solution phenomenon.[28] For oils that exhibit a three-phase region, this problem must be overcome to simulate field performance with an EOS like the Redlich-Kwong. It is relatively easy to extend the

Hand's rule approach to include a third phase.[11,29] With the Redlich-Kwong EOS the simulation of three phases is a more complex task.[28,30]

Displacement of Gas Condensate by Nitrogen

The last problem considered is the nitrogen displacement of a gas condensate. For this problem a 1D displacement is simulated at a temperature of 380 K (224°F) and essentially a constant pressure. The relative permeabilities in Table 2 were again used. The system initially consisted of gas and connate water. The problem was simulated using a 17-component Redlich-Kwong fluid-property description and a three-component description based on Hand's rule. The Redlich-Kwong description was developed from the procedures described by Vogel and Yarborough,[31] but the fluid studied here was not discussed in that paper. The Redlich-Kwong densities and modified Stiel-Thodos viscosity correlation[19] are used throughout. The density correlations described by Vogel and Yarborough were not used because of the inconsistencies that result at a critical point.[6] The Hand's rule description was developed from the Redlich-Kwong description by using the same procedure used for the previous example. In this case, the density and viscosity exponents in Eqs. 16 and 17 were both −0.25.

In Fig. 9, the liquid saturation and overall nitrogen composition profiles are plotted for a displacement at 41.4 MPa (6,000 psi). For this problem, the Hand's rule description agrees reasonably well with the Redlich-Kwong description. With the three-component description, the predicted saturations are somewhat higher early in the displacement and near the inlet. This discrepancy could probably be eliminated by fine-tuning the three-component description.

Fig. 10 is the pseudoternary diagram for this system at 41.4 MPa (6,000 psi). In addition, the phase envelope and critical tie line are plotted for a similar displacement at 34.5 MPa (5,000 psi). If we compare Figs. 8 and 10, it is readily apparent that the simulator predicts a displacement mechanism for this problem that is the same as that for the CO_2-displacement problem. Since the original fluid composition is to the right of the critical tie line and the solvent composition is to the left, the process mechanism is a multiple-contact miscible vaporization one according to the definitions of Hutchinson and Braun.[25] At 34.5 MPa (5,000 psi) the process mechanism is the same as at 41.4 MPa (6,000 psi). However, at a slightly lower pressure the dewpoint of the original fluid is reached. The displacement is immiscible for all pressures below the dewpoint. Even at these low pressures, nitrogen is predicted to vaporize a significant portion of the condensed liquid.

Computational Experience

For the example waterflood problem, the compositional model required 25 seconds on an Intl. Business Machines 3033 to simulate 1.8 displaceable hydrocarbon PV's of injection. An average of 1.08 iterations per timestep were required. On a normalized basis 0.68 milliseconds were required per timestep per gridpoint. The black-oil model used for comparison is based on an IMPES formulation[17] with semi-implicit rate calculations. Although not discussed in the text, the compositional model also uses semi-implicit rates, so that both models have essentially the same stability limit. Timesteps were selected in the two models to make the results as comparable as possible. The black-oil model required 30 seconds overall or 0.65 milliseconds per timestep per gridpoint. This computing time is 20% greater than that required for the compositional model. Overall, this difference is not significant, and the comparison illustrates that the formulations are of comparable efficiency for problems of this type.

Besides the formulation of the solution procedure, the implementation of the Redlich-Kwong EOS has been improved (1) in detecting the transition from one- to two-hydrocarbon phases and (2) in development of a procedure to update the Jacobian elements only when needed.

The details of how these features are incorporated are given in Appendix B, while some test results are presented here. Method 1 for detecting two phase conditions is a variation of the procedure described by Nghiem and Aziz.[32] Method 2 relies on keeping track of the K-values that were found when neighboring gridpoints went two-phase, and using these as initial estimates in a

TABLE 3—TEST RESULTS FOR IMPROVED REDLICH-KWONG EOS IMPLEMENTATION*

	CO_2/Oil	Nitrogen/Gas Condensate		
Case	(13.1 MPa)	(41.4 MPa)	(34.5 MPa)	(31.0 MPa)
1	463	546	795	840
2	436	446	523	840
3	251	296	333	396

*IBM 3033 Computation time (seconds) for 1D flood with 51 gridpoints, 17 components, and 1.2 HCPV injection.

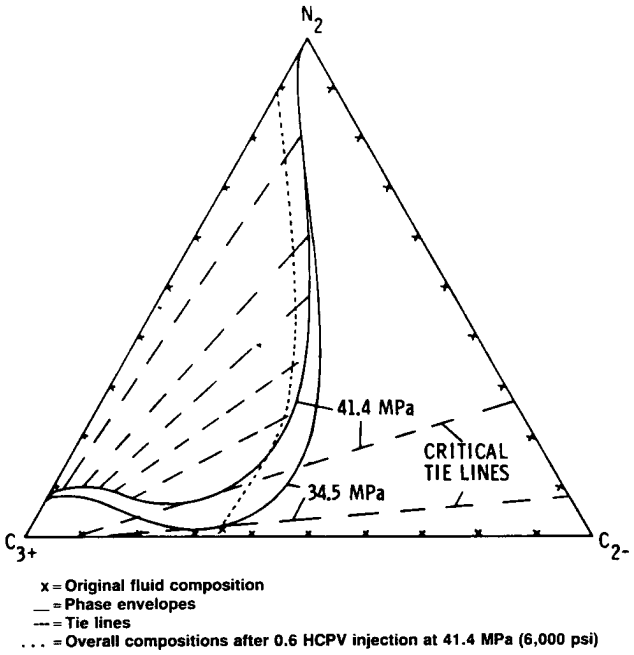

Fig. 10—Ternary diagram of pseudo component mass fractions for displacement of gas condensate with nitrogen.

flash calculation. Table 3 presents results for four different problems—the CO_2-displacement problem and nitrogen displacement of gas condensate at 41.4, 34.5, and 31.0 MPa (6,000, 5,000, and 4,500 psi). The three nitrogen-displacement problems are at respective pressures that are considerably above the dewpoint, slightly above the dewpoint, and below the dewpoint of the original fluid (see Fig. 10). These problems are simulated for three cases: (1) two phases detected by Method 1 and Jacobian-recomputed each iteration, (2) same as Case 1 except two-phase conditions are detected using Method 2, and (3) same as Case 2 except that Jacobian elements are recomputed only at selected gridpoints.

From Table 3, it is apparent that the use of Method 2 to detect two-phase conditions gives a significant reduction in overall computation time. The reduction is greatest when the initial fluid conditions are slightly undersaturated. For the condensate problem at 31 MPa (4,500 psi), no improvement is observed because the initial conditions are in the two-phase region. When the updating of Jacobian elements is based on the criteria described in Appendix B, an even greater reduction in computing time is observed. For the four test problems the average number of iterations per timestep increased from 1.6 for Case 2 to 2.0 for Case 3. This result may suggest that the criteria for recalculation of elements may not be perfect. Nevertheless, the overall computation time decreased an average of 43%. For Case 3, the normalized computing times were, respectively, 11, 12, 13, and 16 milliseconds per timestep per gridpoint.

These improvements have been tested also for 2D and 3D problems, and comparable normalized computing times have been observed. Taking into account machine differences, the computing times for these 17-component problems are two to three times faster than those reported by Nghiem *et al.*[5] for several 10-component problems. The number of iterations they reported differed by roughly this same factor. For a problem involving the displacement of gas condensate by nitrogen in a 2D cross section, the computing time with the formulation described here was 63% less than with the MVNR procedure.[1] These results indicate that the generalized solution procedure when combined with an EOS like the Redlich-Kwong is at least as efficient as any method previously proposed.

For the CO_2-displacement problem, 11.6 seconds of computing time was required for the three-component Hand's rule description and 51 gridpoints to simulate 1.2 hydrocarbon PV's of injection. For the nitrogen-displacement problem at 41.4 MPa (6,000 psi), 13.7 seconds of computation was required with this description method. These times are more than a factor of 20 less than those for Case 3 in Table 3. The simulations averaged 1.00 and 1.02 iterations per timestep, respectively. On a normalized basis, the times were 0.47 and 0.54 milliseconds per timestep per gridpoint, respectively. These normalized times are also representative of multidimensional problems. They are even lower than those observed on the waterflood problem.

It is interesting to note that predictions for miscible gas flooding are often made with black-oil models modified for a first-contact miscible displacement.[33] Since the basic features of the mechanism are not considered with this approach, a great deal of empiricism is often used. The Hand's rule approach at least incorporates the basic features of the process, and the results, just discussed, suggest this can be accomplished with no sacrifice in computer time.

It also is interesting to note that gas condensate and volatile oil reservoirs are often simulated using compositional models and 10 or more components. As a result, great sacrifices in grid resolution are often required. It would appear that the Hand's rule approach (or a generalization of it) is capable of striking a balance between the competing requirements of grid resolution and fluid-property definition.

Conclusions

1. A Newton-Raphson method for solving compositional model equations has been described. This method, when combined with a variety of fluid property correlations, can solve black-oil as well as compositional-type problems efficiently. With this method, no material balance error occurs other than that caused by a lack of machine precision.
2. An improved implementation of a Redlich-Kwong EOS for compositional modeling has been described.
3. Computations have indicated that by using simplified fluid property correlations based on Hand's rule, it may be possible to simulate multiple-contact miscible displacements with only three hydrocarbon-phase components. On a per timestep per gridpoint basis, this scheme gives computation times similar to those of a black-oil model.

Nomenclature

a = coefficients in linearization of Eq. 8
A = block Jacobian elements corresponding to a
B = block Jacobian elements corresponding to Eq. 7
B_g, B_o = reservoir volume factors for gas and oil
c = coefficients in linearization of Eq. 4e
C = block Jacobian elements corresponding to c
d_1, d_2 = tie line slope and intercept parameters for Hand's rule
f_{gi}, f_{oi} = fugacity of component i in light and heavy hydrocarbon phases
F = $\rho_o S_o + \rho_g S_g$, hydrocarbon overall quantity
g = coefficients in linearization of Eq. 3a
G = block Jacobian elements corresponding to g
H = parameter defined by Eq. A-9
J = Jacobian matrix
k = phase permeability, md
K_i = K-value of component i
L = $\rho_o S_o$, heavy hydrocarbon phase quantity
n = number of hydrocarbon phase components
N = total number of grid points
p = pressure, psi (kPa)
q = mass injection rate per unit volume
Q = right-hand side vector in Eq. 7
r = negative of residual vector
R = gas constant
R_s = solution GOR
S = phase saturation

t = time, days
T = flow coefficient array
$\hat{T}$ = temperature, °F (K)
u = composition parameter defined by Eq. A-6 for Hand's rule
v = fraction of hydrocarbon in light phase
v^* = $\rho_g S_g$, light hydrocarbon phase quantity
V_j = PV associated with gridpoint j
V_j' = V_j divided by timestep size
W = $\rho_w S_w$, water phase quantity
x_i = fraction of component i in heavy-hydrocarbon phase
y_i = fraction of component i in light-hydrocarbon phase
z_i = overall fraction of component i
Z = phase compressibility factor
α = exponent in density mixing rule, Eq. 16
γ = exponent in viscosity mixing rule, Eq. 17
δ_{ij} = Kronecker delta
λ = $\rho k/\mu$, phase mobility times density
μ = phase viscosity, cp (Pa·s)
ρ = phase density, lbm/cu ft (kg/m^3)
ρ^* = phase density at surface conditions, lbm/cu ft (kg/m^3)
ϕ = porosity
Ψ = vector of all unknowns combined
$\triangle$ = denotes difference in value over iteration
∇ = gradient operator
$\nabla\cdot$ = divergence operator

Subscripts and Superscripts

f = value associated with overall hydrocarbon
g = value associated with gas or light hydrocarbon
L = value associated with heavy hydrocarbon
m = timestep number
o = value associated with oil or heavy hydrocarbon
p = value associated with pressure
v = value associated with fraction of hydrocarbon in light phase
w = value associated with water
x = value associated with component fractions in heavy-hydrocarbon phase
y = value associated with component fractions in light-hydrocarbon phase
z = value associated with overall component fraction

References

1. Fussell, L.T. and Fussell, D.D.: "An Iterative Technique for Compositional Reservoir Models," *Soc. Pet. Eng. J.* (Aug. 1979) 211-20.
2. Coats, K.H.: "An Equation of State Compositional Model," *Soc. Pet. Eng. J.* (Oct. 1980) 363-76.
3. Roebuck, I.F. *et al.*: "The Compositional Reservoir Simulator: Case 1—The Linear Model," *Soc. Pet. Eng. J.* (March 1969) 115-30; *Trans.*, AIME, **246**.
4. Kazemi, H., Vestal, C.R., and Shank, G.D.: "An Efficient Multicomponent Numerical Simulator," *Soc. Pet. Eng. J.* (Oct. 1978) 355-68.
5. Nghiem, L.X., Fong, D.K., and Aziz, K.: "Compositional Modeling with an Equation of State," *Soc. Pet. Eng. J.* (Dec. 1981) 687-98.
6. Nolen, J.S.: *Numerical Simulation of Compositional Phenomena in Petroleum Reservoirs*, Reprint Series, SPE, Dallas (1973) **11**, 269-84.
7. Redlich, O. and Kwong, J.N.S.: "On the Thermodynamics of Solutions. V. An Equation of State. Fugacities of Gaseous Solutions," *Chem. Reviews* (Feb. 1949) **44**, 233-44.
8. Peng, D.Y. and Robinson, D.B.: "A New Two-Constant Equation of State," *Ind. Eng. Chem. Fund.* (1976) **15**, 59-64.
9. Yarborough, L.: "Application of a Generalized Equation of State to Petroleum Reservoir Fluids," *Equations of State in Engineering*, Advances in Chemistry Series, K.C. Chao and R.L. Robinson (eds.), American Chem. Soc., Washington, D.C. (1979) 385-439.
10. Turek, E.A. *et al.*: "Phase Equilibria in Carbon Dioxide—Multicomponent Hydrocarbon Systems: Experimental Data and Improved Prediction Technique," paper SPE 9231 presented at the 1980 SPE Annual Technical Conference and Exhibition, Dallas, Sept. 21-24.
11. Treybal, R.E.: *Mass Transfer Operations*, McGraw-Hill Book Co., New York City (1968) 29-30.
12. Van-Quy, N., Simandoux, P., and Corteville, J.: "A Numerical Study of Diphasic Multicomponent Flow," *Soc. Pet. Eng. J.* (April 1972) 171-84; *Trans.*, AIME, **253**.
13. Peaceman, D.W.: *Fundamentals of Numerical Reservoir Simulation*, Elsevier Scientific Publishing Co., New York City (1977) 24-27.
14. Young, L.C.: "A Finite-Element Method for Reservoir Simulation," *Soc. Pet. Eng. J.* (Feb. 1981) 115-27.
15. Fussell, D.D. and Yanosik, J.L.: "An Iterative Sequence for Phase Equilibrium Calculations Incorporating the Redlich-Kwong Equation of State," *Soc. Pet. Eng. J.* (June 1978) 173-82.
16. Varga, R.S.: *Matrix Iterative Analysis*, Prentice-Hall, Englewood Cliffs, NJ (1962) 194-99.
17. Aziz, K. and Settari, A.: *Petroleum Reservoir Simulation*, Applied Science Publishers Ltd., London (1979) 135-37.
18. Mansoori, J.: "Discussion of Compositional Modeling With an Equation of State," *Soc. Pet. Eng. J.* (April 1982) 202-03.
19. Lohrenz, J., Bray, B.G., and Clark, C.R.: "Calculating Viscosities of Reservoir Fluids From Their Compositions," *J. Pet. Tech.* (Oct. 1964) 1171-76; *Trans.*, AIME, **231**.
20. Standing, M.B. and Katz, P.L.: "Density of Crude Oils Saturated with Natural Gas," *Trans.*, AIME (1942) **146**, 159-65.
21. Stone, H.L.: "Estimate of Three-Phase Relative Permeability and Residual Oil Data," *J. Cdn. Pet. Tech.* (Oct.-Dec. 1973) 54-61.
22. Thomas, L.K., Lumpkin, W.B., and Reheis, G.M.: "Reservoir Simulation of Variable Bubble-Point Problems," *Soc. Pet. Eng. J.* (Feb. 1976) 10-16; *Trans.*, AIME, **261**.
23. Muskat, M.: *Physical Principles of Oil Production*, McGraw-Hill Book Co. Inc., New York City (1949) 656.
24. Peaceman, D.W.: "Interpretation of Well-Block Pressures in Numerical Reservoir Simulation," *Soc. Pet. Eng. J.* (June 1978) 183-94; *Trans.*, AIME, **265**.
25. Hutchinson, C.A. Jr. and Braun, P.H.: "Phase Relations of Miscible Displacement in Oil Recovery," *AIChE J.* (March 1961) 64-72.
26. Welge, H.J. *et al.*: "The Linear Displacement of Oil From Porous Media by Enriched Gas," *J. Pet. Tech.* (Aug. 1961) 787-96; *Trans.*, AIME, **222**.
27. Helfferich, F.G.: "Theory of Multicomponent, Multiphase Displacement in Porous Media," *Soc. Pet. Eng. J.* (Feb. 1981) 51-62.
28. Baker, L.E., Pierce, A.C., and Luks, K.D.: "Gibbs Energy Analysis of Phase Equilibria," *Soc. Pet. Eng. J.* (Oct. 1982) 731-42.
29. Gardner, J.W., Orr, F.M., and Patel, P.D.: "The Effect of Phase Behavior on CO_2 Flood Displacement Efficiency," *J. Pet. Tech.* (Nov. 1981) 2067-81.
30. Fussell, L.T.: "A Technique for Calculating Multiphase Equilibria," *Soc. Pet. Eng. J.* (Aug. 1979) 203-08.
31. Vogel, J.L. and Yarborough, L.: "The Effect of Nitrogen on the Phase Behavior and Physical Properties of Reservoir Fluids," paper SPE 8815 presented at the 1980 SPE/DOE Joint Enhanced Oil Recovery Symposium, Tulsa, April 20-23.
32. Nghiem, L.X., Aziz, K., and Li, Y.K.: "A Robust Iterative Method for Flash Calculations Using the Soave-Redlich-Kwong or

the Peng-Robinson Equation of State," *Soc. Pet. Eng. J.* (June 1983) 521-30.
33. Lantz, R.B.: "Rigorous Calculation of Miscible Displacement Using Immiscible Reservoir Simulators," *Soc. Pet. Eng. J.* (June 1970) 192-202; *Trans.*, AIME, **249**.
34. Baker, L.E. and Luks, K.D.: "Critical Point and Saturation Pressure Calculation for Multicomponent Systems," *Soc. Pet. Eng. J.* (Feb. 1980) 15-24.

APPENDIX A
Linearization of Equations for *K*-Values Dependent on Pressure and Overall Composition

For systems obeying this assumption, Eqs. 3b, 4c, and 5 can be used to express as functions of p, v, and z_i, $i=i \ldots n-1$ the quantities

$$z_n=1-\sum_{i=1}^{n-1} z_i, \quad \ldots\ldots\ldots\ldots\ldots\ldots\ldots\ldots\ldots\ldots (A\text{-}1)$$

$$x_i=z_i/[1+(K_i-1)v], \quad \ldots\ldots\ldots\ldots\ldots\ldots\ldots (A\text{-}2)$$

and

$$y_i=K_i z_i/[1+(K_i-1)v], \quad \ldots\ldots\ldots\ldots\ldots\ldots\ldots (A\text{-}3)$$

$i=1 \ldots n$. The linearization of Eqs. 4e and 8 are first derived for the case in which K-values are strictly a function of pressure, and then for a three-component system obeying Hand's rule.

K-Values Dependent on Pressure

For the case with K-values a function of pressure only, the following derivatives are used to linearize Eq. 8:

$$\frac{\partial}{\partial v}\left[\sum_{i=1}^{n}(y_i-x_i)\right]=-\sum_{i=1}^{n}\frac{(y_i-x_i)^2}{z_i}=a_v,$$

$$\frac{\partial}{\partial p}\left[\sum_{i=1}^{n}(y_i-x_i)\right]=\sum_{i=1}^{n}x_i\left(\frac{x_i}{z_i}\right)\frac{dK_i}{dp}=a_p,$$

and

$$\frac{\partial}{\partial z_i}\left[\sum_{j=1}^{n}(y_j-x_j)\right]=\frac{y_i}{z_i}-\frac{x_i}{z_i}-\frac{y_n}{z_n}+\frac{x_n}{z_n}=a_i,$$

$$i=1 \ldots n-1. \quad \ldots\ldots\ldots\ldots\ldots\ldots\ldots (A\text{-}4)$$

To linearize (Eq. 4e) requires the derivatives

$$\frac{\partial}{\partial v}(1-S_o-S_g-S_w)=F\left(\frac{1}{\rho_o}-\frac{1}{\rho_g}\right)$$

$$-F(1-v)\frac{\partial}{\partial v}\left(\frac{1}{\rho_o}\right)-Fv\frac{\partial}{\partial v}\left(\frac{1}{\rho_g}\right)=c_v,$$

$$\frac{\partial}{\partial p}(1-S_o-S_g-S_w)=-F\left[(1-v)\frac{\partial}{\partial p}\left(\frac{1}{\rho_o}\right)+v\frac{\partial}{\partial p}\left(\frac{1}{\rho_g}\right)\right]-W\frac{\partial}{\partial p}\left(\frac{1}{\rho_w}\right)=c_p,$$

and

$$\frac{\partial}{\partial z_i}(1-S_o-S_g-S_w)=-F\left[(1-v)\frac{\partial}{\partial z_i}\left(\frac{1}{\rho_o}\right)+v\frac{\partial}{\partial z_i}\left(\frac{1}{\rho_g}\right)\right]=c_i. \quad (A\text{-}5)$$

The derivatives with respect to F and W are as indicated in Eq. 13. Derivatives of ρ_o and ρ_g are needed in Eq. A-5. To obtain these derivatives, Eq. 16 is differentiated with respect to p, x_i, and y_i, while Eqs. A-1, A-2, and A-3 are differentiated with respect to p, v, and z_i. The chain rule is then applied to calculate the derivatives of ρ_o and ρ_g with respect to p, v, and z_i for $i=1 \ldots n$. These expressions are then used in Eq. A-5.

These expressions simplify considerably for gridpoints that are in a single-phase hydrocarbon state. This condition can be detected readily by

$$v=0 \text{ if } \sum_{i=1}^{n} K_i z_i<1,$$

and

$$v=1 \text{ if } \sum_{i=1}^{n} z_i/K_i<1.$$

For either of these conditions, Eq. 9 reduces to

$$\Delta v=0.$$

The coefficients in Eq. 11 are readily calculated, since the overall composition is equivalent to the composition of the phase that is present.

Hand's Rule

Hand's rule is a tie-line relationship that assumes that for a ternary system all tie lines intersect at a given point. Van-Quy *et al.*[12] point out that this assumption allows the composition variable u to be defined as

$$u=\frac{z_1}{d_1(p)z_2+d_2(p)}, \quad \ldots\ldots\ldots\ldots\ldots\ldots (A\text{-}6)$$

such that $d_1 u$ and $d_2 u$ are the slope and intercept of the tie-line corresponding to the given overall composition and pressure. For convenience u is normalized to a value of unity on the critical tie line. The liquid and vapor compositions lie on the tie line—i.e.,

$$x_1=u(d_1 x_2+d_2),$$

and

$$y_1 = u(d_1 y_2 + d_2). \quad \ldots\ldots\ldots\ldots\ldots\ldots\ldots\ldots \text{(A-7)}$$

Two K-values are assumed to be functions of u and p, given by

$$K_2 = K_2(u,p)$$

and

$$K_3 = K_3(u,p). \quad \ldots\ldots\ldots\ldots\ldots\ldots\ldots\ldots \text{(A-8)}$$

The first K-value is indirectly specified by Eqs. A-7. Eq. 8 is replaced by the equivalent relationship

$$H = (d_1 u + 1)(K_2 - 1)z_2 + (K_3 - 1)(1 - z_1 - z_2)$$

$$+ (K_2 - 1)(K_3 - 1)(1 - d_2 u)v = 0. \quad \ldots\ldots\ldots \text{(A-9)}$$

Eq. A-9 is linearized by first differentiating H with respect to u, v, p, z_1, and z_2. u is then eliminated by differentiation of Eq. A-6 and by application of the chain rule.

Eq. A-5 applies equally for Hand's rule. The derivatives of ρ_o and ρ_g are calculated in an analogous fashion.

Gridpoints with only a single hydrocarbon phase can be detected in one of two ways. If Eq. A-6 indicates a value of $u > 1$, then a dense phase condition is present. If Eq. A-6 indicates a value of $u < 1$, then a single-phase state can be determined by solving Eq. A-9 for v. If Eq. A-9 indicates a value < 0 or > 1, then only a single phase exists.

For a single-phase condition, the linearized equations are determined by using the procedure described for the case with K-values a function of pressure only.

APPENDIX B

Linearization of Equations for Phase Equilibria a Function of Individual Phase Compositions

For systems of this type, Eqs. 4a and 4b are rearranged as

$$x_n = 1 - \sum_{i=1}^{n-1} x_i, \quad \ldots\ldots\ldots\ldots\ldots\ldots\ldots \text{(B-1)}$$

and

$$y_n = 1 - \sum_{i=1}^{n-1} y_i. \quad \ldots\ldots\ldots\ldots\ldots\ldots\ldots \text{(B-2)}$$

The fugacities and compressibility factors of both phases can be differentiated and the above constraints applied to determine the quantities

$$\frac{\partial Z_o}{\partial x_j}, \frac{\partial Z_g}{\partial y_j}, \frac{\partial f_{oi}}{\partial x_j}, \frac{\partial f_{gi}}{\partial y_j}, \frac{\partial Z_o}{\partial p}, \frac{\partial Z_g}{\partial p}, \frac{\partial f_{oi}}{\partial p}, \frac{\partial f_{gi}}{\partial p},$$

$i = 1 \ldots n$; $j = 1 \ldots n-1$. The x_i can then be expressed by using Eq. 5 as

$$x_i = \frac{z_i - v y_i}{1 - v}; \quad i = 1 \ldots n-1. \quad \ldots\ldots\ldots\ldots \text{(B-3)}$$

By differentiating Eq. B-3 and using the chain rule, the following derivatives can be used to linearize Eq. 3a in terms of y_i, z_i, $i = 1 \ldots n-1$, v, and p:

$$(1-v)\frac{\partial}{\partial y_j}(f_{oi} - f_{gi}) = -v\frac{\partial f_{oi}}{\partial x_j} - (1-v)\frac{\partial f_{gi}}{\partial y_j} = g_{yij},$$

$$(1-v)\frac{\partial}{\partial z_j}(f_{oi} - f_{gi}) = \frac{\partial f_{oi}}{\partial x_j} = g_{zij},$$

$$(1-v)\frac{\partial}{\partial v}(f_{oi} - f_{gi}) = \sum_{j=1}^{n-1} \frac{\partial f_{oi}}{\partial x_j}(x_j - y_j) = g_{vij},$$

and

$$(1-v)\frac{\partial}{\partial p}(f_{oi} - f_{gi}) = (1-v)\left[\frac{\partial f_{oi}}{\partial p} - \frac{\partial f_{gi}}{\partial p}\right] = g_{pij}.$$

$$\ldots\ldots\ldots\ldots\ldots\ldots\ldots\ldots\ldots\ldots\ldots\ldots\ldots\ldots \text{(B-4)}$$

The residuals and Jacobian are scaled by the factor $(1-v)$ to avoid ill-conditioning when v approaches unity. This scaling alleviates the need to switch to an L-x iteration when v is near unity.

The saturation constraint equation, Eq. 4d or 4e, can be written in terms of compressibility factors as

$$1 - F[(1-v)Z_o + vZ_g]\left(\frac{R\hat{T}}{p}\right) - \frac{W}{\rho_w} = 0. \quad \ldots\ldots \text{(B-5)}$$

This equation can be linearized by using the derivatives

$$\frac{\partial}{\partial y_i}(1 - S_o - S_g - S_w) = Fv\left(\frac{R\hat{T}}{p}\right)\left(\frac{\partial Z_o}{\partial x_i} - \frac{\partial Z_g}{\partial y_i}\right)$$

$$= c_{yi},$$

$$\frac{\partial}{\partial z_i}(1 - S_o - S_g - S_w) = -F\left(\frac{R\hat{T}}{p}\right)\frac{\partial Z_o}{\partial x_i} = c_i,$$

$$\frac{\partial}{\partial v}(1 - S_o - S_g - S_w) = F\left(\frac{R\hat{T}}{p}\right)\left[(Z_o - Z_g)\right.$$

$$\left. - \sum_{i=1}^{n-1}(x_i - y_i)\frac{\partial Z_o}{\partial x_i}\right] = c_v,$$

and

$$\frac{\partial}{\partial p}(1-S_o-S_g-S_w)$$

$$=F\left(\frac{R\hat{T}}{p}\right)\left[(1-v)\left(\frac{Z_o}{p}-\frac{\partial Z_o}{\partial p}\right)\right.$$

$$\left.+v\left(\frac{Z_g}{p}-\frac{\partial Z_g}{\partial p}\right)\right]-W\frac{\partial}{\partial p}\left(\frac{1}{\rho_w}\right)=c_p. \quad \ldots\ldots \text{(B-6)}$$

The derivatives with respect to F and W are as indicated in Eq. 13.

For a compositional model, a major amount of the computations are spent calculating and eliminating the derivatives just described. A great deal of this time can be saved if these Jacobian elements are recalculated only when needed. We have successfully used a procedure whereby the elements are calculated and eliminated only for gridpoints that do not meet the convergence tolerance. For gridpoints meeting the tolerance, only the residuals need to be calculated and eliminated. With this procedure, gridpoints at which no changes are occurring may pass for several timesteps without recalculation of the Jacobian. Significant reductions in computation time have been observed with this approach.

Detection of the Two-Phase Region

Detecting the conditions when a gridpoint passes from a single-hydrocarbon-phase state to one having two hydrocarbon phases can be a difficult and time-consuming problem for compositional models that employ an EOS such as the Redlich-Kwong or Peng-Robinson. Two basic procedures have been proposed to accomplish this task. They are based on (1) keeping track of the saturation pressure at each gridpoint and comparing this to the gridpoint pressure, and (2) performing a flash calculation to determine whether a two-phase solution exists.

Baker and Luks[34] describe the only procedure of the first type that has proved to be reliable. This procedure is time-consuming, and for oils that exhibit a three-phase region, it fails because of the multiple-solution phenomenon.[28] Nghiem *et al.*[5,32] used a procedure of the second type. They performed the flash calculation by using successive substitution iterations initially and by switching to Powell's method near the solution. We have tried this basic technique except that we switch to a Newton-Raphson iteration rather than Powell's method. We found that the technique occasionally fails to detect a two-phase condition because of poor initial K-value estimates. The procedure can be made to work if the K-value of the solvent component is set initially to a large value (e.g., 10^{10}). This prevents the erroneous prediction of a single-phase condition at the beginning of the iteration sequence. We designate as Method 1 the procedure of Nghiem *et al.*, with the modifications just described.

We have also had good success with another procedure of the second type. The method is based on the idea that since neighboring cells experience similar composition histories, a good source of initial K-value estimates should be given by the neighboring gridpoints that have previously experienced a phase transition. When a gridpoint becomes two-phase, the K-values found are transferred to neighboring gridpoints. These K-values are used initially in an iteration sequence like that described above. With the exception of wellpoints, gridpoints that have no two-phase neighbors are not tested. At wellpoints Method 1 is used. The procedure just described is designated as Method 2.

SI Metric Conversion Factors

psi × 6.894 757 E+00 = kPa

*Conversion factor is exact.

SPEJ

Original manuscript received in Society of Petroleum Engineers office Oct. 27, 1981. Paper accepted for publication Feb. 7, 1983. Revised manuscript received May 2, 1983. Paper (SPE 10516) first presented at the 1982 SPE Reservoir Simulation Symposium held in New Orleans, Jan. 31–Feb. 3.